

The radial disc structure around a magnetic neutron star: analytic and semi-analytic solutions

Axel Brandenburg and Chris G. Campbell

Department of Mathematics, University of Newcastle upon Tyne, NE1 7RU

Accepted 1998 March 3. Received 1997 November 27; in original form 1997 October 14

ABSTRACT

The radial structure of a thin accretion disc is calculated in the presence of a central dipole magnetic field aligned with the rotation axis. The problem is treated using a modified expression for the turbulent magnetic diffusion, which allows the angular momentum equation to be integrated analytically. The governing algebraic equations are solved iteratively between 1 and 10^4 stellar radii. An analytic approximation is provided that is valid near the disruption radius at about 100 stellar radii. At that point, which is approximately 60 per cent of the Alfvén radius and typically about 30 per cent of the corotation radius, the disc becomes viscously unstable. This instability results from the fact that both radiation pressure and opacity caused by electron scattering become important. This in turn is a consequence of the magnetic field which leads to an enhanced temperature in the inner parts. This is because the magnetic field gives rise to a strongly enhanced vertically integrated viscosity, so that the viscous torque can balance the magnetic torque.

Key words: accretion, accretion discs – magnetic fields – stars: neutron.

1 INTRODUCTION

Accretion discs occur around strong magnetic stars in X-ray binary pulsars (Verbunt 1993), intermediate polar binaries (Warner 1995) and T Tauri stars (Basri & Bertout 1989). The stellar magnetic field interacts with the disc, significantly modifying its structure in its inner regions, and this in turn affects the spin evolution of the star. The early work on the problem is discussed in Campbell (1997). Campbell (1992) gave an analytic, *reductio ad absurdum* proof that, for realistic magnetic diffusivities, the disc cannot exist over a significant radial extent with $|F_{m\phi}|$ much larger than $|F_{v\phi}|$, where \mathbf{F}_m and \mathbf{F}_v are the magnetic and viscous forces. Recently, Heptinstall (1997) and Campbell & Heptinstall (1998) numerically integrated the magnetic disc equations throughout the disc. They found that the magnetic field causes the disc temperature to be elevated in its inner regions above values in an unperturbed disc. This causes the electron scattering opacity and radiation pressure to become important further from the star. When the radiation pressure becomes comparable to the gas pressure the density reaches a maximum and slightly closer to the star viscous instability occurs. Simultaneously the vertical scaleheight diverges as the disc ends. This work employed simple forms of magnetic diffusivity to represent the effects of turbulence and magnetic buoyancy.

The present paper uses a form of magnetic diffusivity which enables more analytic progress to be made. In Section 2 the governing equations are presented, while in Section 3 an analytic solution is found for the vertically integrated viscosity function $\nu\Sigma$. The resulting non-linear, algebraic set of equations is solved in Section 4 and the solutions are presented. In Section 5 an analytic

solution is found valid close to the turnover radius in the density. Sections 6 and 7 consider the sensitivity of the solutions to the form of magnetic diffusivity used and the effects of vertical mass transfer, respectively. The results are discussed in Section 8.

2 GOVERNING EQUATIONS

In the thin-disc approximation the radial structure of a disc threaded by a vertical magnetic field is governed by the equations of angular momentum balance, vertical equilibrium and thermal equilibrium. For the detailed derivation of the relevant equations we refer to the original work of Campbell (1992), Heptinstall (1997) and Campbell & Heptinstall (1998); see also the monograph by Campbell (1997). Here, we restrict ourselves to a brief discussion of the additional terms that were added to the standard (non-magnetic) thin-disc equations.

We assume that the dipole magnetic field is aligned with the rotation axis. Hence, in the equatorial plane of the disc the magnetic field of the central neutron star is, in the absence of a disc, vertical and equal to

$$B_z = -\frac{B}{2} \left(\frac{R}{\varpi} \right)^3, \quad (1)$$

where B is the polar field strength at the surface of the star, R is its radius, and ϖ is the cylindrical radius. The magnetic field of the star rotates with the angular velocity of the star, $\Omega_s = 2\pi/P$, where P is its rotation period. The shear resulting from the difference between Ω_s and the Keplerian angular velocity in the disc, $\Omega_K = (GM/\varpi^3)^{1/2}$ produces a toroidal magnetic field in the disc. The

toroidal field B_ϕ changes sign about the midplane. For the value of B_ϕ at $z = h$, where h is the density scaleheight, Campbell (1992) found

$$B_\phi^+ = -\frac{\gamma \varpi B_z}{\eta} (\Omega_K - \Omega_s) h, \quad (2)$$

where η is the turbulent magnetic diffusivity and $\gamma < 1$ is a dimensionless parameter to account for a reduction in the vertical shear due to magnetospheric poloidal flows. This parameter could account for enhanced η values due to dynamical instabilities precipitated by large vertical shear.

With these preparations we can now write down the three governing equations for the three unknowns h (disc height or semithickness), $\Sigma = \rho_c h$ (surface density), and T_c (temperature at the central plane) for a thin disc in the presence of an imposed vertical magnetic field (Heptinstall 1997; Campbell & Heptinstall 1998). We have

$$-\frac{\dot{M}}{4\pi} \frac{d}{d\varpi} (\varpi^2 \Omega_K) = \frac{d}{d\varpi} \left(\frac{1}{2} \nu \rho_c h \varpi^3 \frac{d\Omega_K}{d\varpi} \right) + \varpi^2 \frac{B_z B_\phi^+}{\mu_0}, \quad (3)$$

$$\frac{1}{2} \rho_c \Omega_K^2 h^2 + \frac{(B_\phi^+)^2}{2\mu_0} - P_c = 0, \quad (4)$$

$$\frac{4\sigma T_c^4}{3\kappa \rho_c h} = \frac{\eta (B_\phi^+)^2}{h \mu_0} + \frac{9}{8} \nu \rho_c h \Omega_K^2, \quad (5)$$

where P_c is the pressure at the central plane. It consists of gas and radiative pressures, so

$$P_c = P_{\text{gas}} + P_{\text{rad}} = \frac{\mathcal{R} T_c}{\mu_{\text{gas}}} \rho_c + \frac{4\sigma}{3c} T_c^4. \quad (6)$$

Here, $\mathcal{R} = 8315 \text{ m}^2 \text{ s}^{-2} \text{ K}^{-1}$ is the fundamental gas constant, $\mu_{\text{gas}} \approx 0.62$ the mean molecular weight, $\sigma = 5.67 \times 10^{-8} \text{ J m}^{-2} \text{ s}^{-1} \text{ K}^{-4}$ the Stefan–Boltzmann constant, and $c = 3 \times 10^8 \text{ m s}^{-1}$ the speed of light. For the opacity κ we include free–free and bound–free transitions (Kramers opacity κ_{Kr}) and electron scattering (κ_{es}), so

$$\kappa = \kappa_{\text{Kr}} + \kappa_{\text{es}} = \kappa_0 \rho_c T_c^{-7/2} + 0.02(1 + X) \text{ m}^2 \text{ kg}^{-1}. \quad (7)$$

We adopt the value $X = 0.6625$ for the hydrogen abundance, consistent with Heptinstall (1997). (We checked, however, that the results presented below are unchanged if we take $X = 0.7$.) For the constant κ_0 we adopt the value $5 \times 10^{20} \text{ m}^5 \text{ kg}^{-2} \text{ K}^{7/2}$, which gave fair agreement with a numerical table in the parameter range of interest.

As mentioned earlier, it is possible to integrate the angular momentum equation in closed form provided one assumes a suitable turbulent diffusivity prescription. The standard recipe is to approximate a turbulent diffusion coefficient by some mean free path (or rather some correlation length) of the turbulence times some typical transport velocity. The typical velocity is some fraction of the sound speed c_s (which is $\Omega_K h$ for thin accretion discs). The correlation length is assumed to be some fraction of the disc height h . So, for the viscosity we then adopt the usual Shakura–Sunyaev prescription

$$\nu = \alpha \Omega_K h^2, \quad (8)$$

where $\alpha < 1$ is a free parameter. For the magnetic diffusivity we adopt a slightly different prescription,

$$\eta = \epsilon \Omega_K h \varpi, \quad (9)$$

the advantages of which will become clear in the next section. This prescription is taken for analytical convenience, but in practice the

formulation hardly differs from the more obvious alternative similar to (8). We return to this issue in Section 6. With this prescription for η we effectively measure the correlation length in fractions of the cylindrical radius rather than the disc height. However, the ratio between the two is almost constant. (For the Shakura–Sunyaev solution $h/\varpi \sim \varpi^{1/8}$.) Our prescription is therefore not only a sensible hypothesis, but also a good approximation to the Shakura–Sunyaev-like approach, which was used by Heptinstall (1997) and Campbell & Heptinstall (1998). The magnetic Prandtl number, which is the ratio between the two diffusion coefficients,

$$\text{Pr}_M \equiv \frac{\nu}{\eta} = \frac{\alpha h}{\epsilon \varpi} \quad (10)$$

depends only weakly on ϖ . Typically, $h/\varpi \approx 0.01$, so in order to have $\text{Pr}_M \approx 1$ we have to choose $\epsilon/\alpha = 0.01$. Our fiducial set of parameters adopted below is consistent with that used by Heptinstall (1997) and Campbell & Heptinstall (1998): $M = 1.4 M_\odot$, $\dot{M} = 10^{-9} M_\odot \text{ yr}^{-1}$, $P = 10 \text{ s}$, $R = 10^4 \text{ m}$, $B = 10^8 \text{ T} (= 10^{12} \text{ G})$, $\alpha = 10^{-2}$, $\epsilon = 10^{-4}$ and $\gamma = 10^{-2}$.

3 INTEGRATING THE ANGULAR MOMENTUM EQUATION

Consider first the vertical Maxwell stress in equation (3) and eliminate B_ϕ^+ using equation (2), so

$$\varpi^2 \frac{B_z B_\phi^+}{\mu_0} = -\varpi^3 \frac{B_z^2 \gamma}{\mu_0 \eta} (\Omega_K - \Omega_s) h, \quad (11)$$

where

$$\Omega_K = \sqrt{GM} \varpi^{-3/2} \quad \text{and} \quad \Omega_s = \sqrt{GM} \varpi_{\text{co}}^{-3/2} \quad (12)$$

are the Keplerian angular velocity and the angular velocity of the star, respectively. The latter is here defined in terms of the corotation radius,

$$\varpi_{\text{co}} = (GM/\Omega_s^2)^{1/3} = \left[GM \left(\frac{P}{2\pi} \right)^2 \right]^{1/3}. \quad (13)$$

Thus, we have

$$\varpi^2 \frac{B_z B_\phi^+}{\mu_0} = -\varpi^3 \frac{B_z^2 \gamma}{\mu_0 \eta} \Omega_K \left[1 - \left(\frac{\varpi}{\varpi_{\text{co}}} \right)^{3/2} \right] h. \quad (14)$$

Using equations (1) and (9) we can now write

$$\varpi^2 \frac{B_z B_\phi^+}{\mu_0} = \frac{d}{d\varpi} \left\{ \varpi^{-3} \frac{R^6 B^2 \gamma}{6 \cdot 2\mu_0} \left[1 - 2 \left(\frac{\varpi}{\varpi_{\text{co}}} \right)^{3/2} \right] \right\}. \quad (15)$$

Substituting equation (15) into equation (3) and integrating we have

$$\frac{\dot{M}}{4\pi} \varpi^2 \Omega_K + \frac{1}{2} \nu \rho_c h \varpi^3 \frac{d\Omega_K}{d\varpi} + \varpi^{-3} \frac{R^6 B^2}{6 \cdot 2\mu_0} \frac{g(\varpi)}{\hat{\epsilon}} = C, \quad (16)$$

where C is an integration constant, $\hat{\epsilon} = \epsilon/\gamma$ and

$$g(\varpi) = 1 - 2 \left(\frac{\varpi}{\varpi_{\text{co}}} \right)^{3/2}. \quad (17)$$

In the standard Shakura–Sunyaev solution C is derived from the condition that very near the stellar surface $\Omega = \Omega_s$, and so Ω must go through a maximum, i.e. $d\Omega/d\varpi = 0$ at $\varpi = R$. Thus, C would follow from (16) by putting $d\Omega/d\varpi = 0$ and $\varpi = R$. However, a similar procedure cannot be applied in the present case for two reasons. First, the disc does not extend down to $\varpi = R$ and secondly, at the point where the disc ends the rotation of the disc is still almost Keplerian. On the other hand, we want to ensure that for very large radii the disc structure matches that of the

Shakura–Sunyaev solution. This requires that the effect of C must become negligible at large radii. Therefore we assume $C = 0$. A more consistent treatment could be adopted by matching to a known solution for the magnetospheric flow.

Using $d\Omega_K/d\varpi = -(3/2)(\Omega_K/\varpi)$, $\Sigma = \rho_c h$, dividing by $\frac{3}{4}\varpi^2\Omega_K$, and rearranging the equation such that the viscous term appears on the left-hand side, we arrive at

$$\nu\Sigma = \frac{\dot{M}}{3\pi} + \frac{2R^3}{9\varpi^2\Omega_K} \frac{B^2}{2\mu_0} \left(\frac{R}{\varpi}\right)^3 \frac{g(\varpi)}{\hat{\epsilon}}. \quad (18)$$

It is convenient to define the integrated viscosity, $\mu = \nu\Sigma$, and to write equation (18) in the form

$$\mu = \frac{\dot{M}}{3\pi} F, \quad (19)$$

where

$$F = 1 + \frac{2R^3}{9\varpi^2\Omega_K} \frac{3\pi B^2}{\dot{M} 2\mu_0} \left(\frac{R}{\varpi}\right)^3 \frac{g(\varpi)}{\hat{\epsilon}}. \quad (20)$$

Again, we write $\Omega_K = \Omega_s(\varpi/\varpi_{co})^{-3/2}$ and express Ω_s in terms of the stellar rotation period $P = 2\pi/\Omega_s$, so we have

$$F = 1 + \left(\frac{R}{\varpi}\right)^5 \left(\frac{\varpi}{\varpi_{co}}\right)^{3/2} \frac{RP}{3\dot{M} 2\mu_0} \frac{B^2 g(\varpi)}{\hat{\epsilon}}. \quad (21)$$

This can be rewritten in terms of the spherical Alfvén radius

$$\varpi_A = \left(\frac{\sqrt{2\pi R^6 B^2}}{\sqrt{GM\mu_0}}\right)^{2/7}. \quad (22)$$

Thus, we can write

$$F = 1 + \frac{1}{3\sqrt{2}} \left(\frac{\varpi_A}{\varpi}\right)^{7/2} \frac{g(\varpi)}{\hat{\epsilon}}. \quad (23)$$

The result for $\mu = \mu(\varpi)$ is given in Fig. 1 and compared with the non-magnetic case.

For $\varpi < \varpi_A$, the second term in equation (23) dominates and the solution can be approximated by

$$\mu \approx 6.5 \times 10^{15} \times \hat{\epsilon}_{-2}^{-1} \varpi_6^{-7/2} R_4^6 B_8^2 M_{1.4}^{-1/2} \text{ kg s}^{-1}, \quad (24)$$

where ϖ_6 is the cylindrical radius measured in 10^6 m, $\hat{\epsilon}_{-2} = \hat{\epsilon}/0.01$, R_4 is the radius of the central object in 10^4 m, B_8 the dipole field strength at the stellar surface in 10^8 T, and $M_{1.4}$ the central mass in units of $1.4 M_\odot$. It is remarkable that ϖ_{co} drops out and that neither P nor \dot{M} enters this asymptotic expression for μ . This means that the spherical Alfvén radius does not provide a meaningful parametrization of the disruption radius. The rotation period of the star does enter the problem, however, through the term $g(\varpi)/\hat{\epsilon}$ in equation (23). This term may change sign, so that F could become negative well outside the corotation radius. In that case there is obviously no

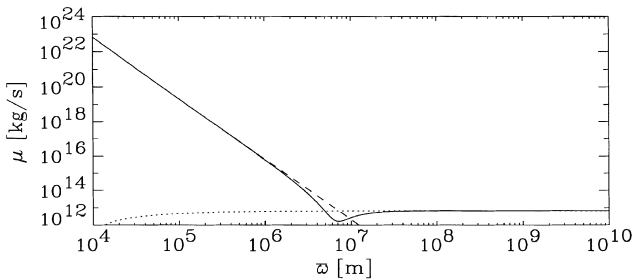


Figure 1. Solid line: $\mu = \mu(\varpi)$ for $\dot{M} = 10^{-9} M_\odot \text{ yr}^{-1}$. The dotted line refers to the Shakura–Sunyaev solution and the dashed line to the magnetically dominated solution.

solution for μ . For our fiducial set of parameters this happens for a rotation period of less than around 7 s. However, with larger values of $\hat{\epsilon}$ the second term in (23) can always be made small enough that positive solutions for μ become possible again.

It is important to realize that equation (24) implies that in the inner regions the magnetic stress very nearly balances the viscous stress – not the Reynolds stress due to radial advection, as it is sometimes assumed.

We note that we have used the dipolar form (1) for B_z . Bardou & Heyvaerts (1996) argue that when $|B_\phi^+|/|B_z| \gg 1$ the poloidal field is liable to inflate. The resulting poloidal field is still largely vertical in and near the disc, but has a different radial dependence from a dipole field. However, as explained in Campbell & Heptinstall (1998), poloidal flows are likely in the magnetosphere and these reduce the vertical shear across the disc. This leads to smaller values of $|B_\phi^+|/|B_z|$, corresponding to $\gamma < 1$ in (2). In the present paper the field ratio is given by (14) as

$$\frac{|B_\phi^+|}{|B_z|} = \gamma \frac{\Omega_K \varpi h}{\eta} \left[1 - \left(\frac{\varpi}{\varpi_{co}}\right)^{3/2} \right] \approx \frac{\gamma}{\epsilon}, \quad (25)$$

where the last expression follows from the use of (9) for η . Hence when $\gamma/\epsilon \sim 1$ it follows that $|B_\phi^+|/|B_z| \sim 1$ and inflation will not occur. This justifies our use of (1) for B_z .

4 ITERATIVE SOLUTION FOR THE DISC STRUCTURE

Equation (19) gives the viscosity integral $\mu \equiv \nu\Sigma$ for given \dot{M} , B and other parameters as a function of ϖ . In a more general situation, when the system is time-dependent, there is no fixed \dot{M} , and equation (19) has to be replaced by an explicitly time-dependent diffusion-type equation for Σ . In any case, in order to close the system of equations we need another equation that relates μ to Σ . In the time-dependent case the sign of $\partial\mu/\partial\Sigma$ determines whether the solution is viscously stable (positive sign) or unstable (negative sign). In the steady case we calculate $\Sigma = \Sigma(\mu)$, where μ has been calculated in the previous section. Because of the presence of additive variables the equations are no longer linear in the logarithms of the various variables, as is the case in the Shakura–Sunyaev theory. Therefore we have to iterate with respect to the additive corrections resulting from the presence of the magnetic field, radiation pressure and the contribution from the Kramers opacity.

We now derive the equation $\Sigma = \Sigma(\mu)$ from equations (4) and (5). We begin with equations (4) and (6), which we rewrite in the form

$$T_c = \frac{1}{2}\Omega_K^2 h^2 \frac{1 + \beta^{-1}}{1 + \beta_r^{-1}} \frac{\mu}{\mathcal{R}}, \quad (26)$$

where we have defined

$$\beta^{-1} = \frac{(B_\phi^+)^2}{2\mu_0 \rho_c \Omega_K^2 h^2} \quad (27)$$

as the inverse plasma beta, which is the ratio of magnetic to gas pressure, and

$$\beta_r^{-1} = \frac{\mu}{\mathcal{R}} \frac{4\sigma T_c^3}{3c \rho_c}, \quad (28)$$

which is the ratio of radiation to gas pressure. The toroidal magnetic field is just a function of ϖ (in particular independent of h !), because we have assumed $\eta = \epsilon\Omega_K h\varpi$. Thus,

$$B_\phi^+ = -\frac{1}{2}B \left(\frac{R}{\varpi}\right)^3 \frac{\gamma}{\epsilon} \left[1 - \left(\frac{\varpi}{\varpi_{co}}\right)^{3/2} \right]; \quad (29)$$

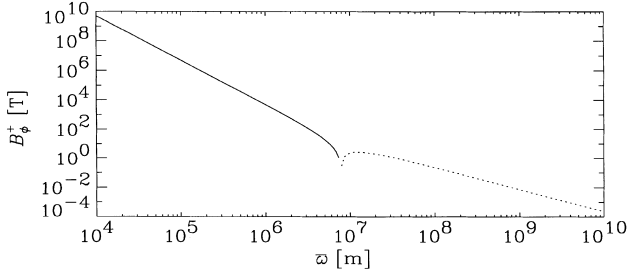


Figure 2. $B_\phi = B_\phi(\varpi)$ for $B = 10^8$ T. The dotted line refers to negative values of $B_\phi(\varpi)$.

see Fig. 2. Note the change of sign and slope near the corotation radius.

Another relation between T_c and the other variables can be obtained from equation (5) after using the opacity law

$$T_c^4 = \frac{27\kappa_{es}}{32\sigma} \alpha \Sigma^2 h^2 \Omega_K^3 \left(1 + \frac{16}{9} \text{Pr}_M^{-1} \beta^{-1}\right) \left(1 + \frac{\kappa_{Kr}}{\kappa_{es}}\right). \quad (30)$$

We combine this with equation (26) to eliminate T_c , and arrive after some simplifications at

$$h^6 = \mathcal{K} \alpha \Sigma^2 \Omega_K^{-5} C, \quad (31)$$

where we have defined

$$\mathcal{K} = \frac{27\kappa_{es}}{2\sigma} \left(\frac{\mathcal{R}}{\mu}\right)^4 \quad (32)$$

and the function

$$C = \left(1 + \frac{16}{9} \text{Pr}_M^{-1} \beta^{-1}\right) \left(\frac{1 + \beta_r^{-1}}{1 + \beta^{-1}}\right)^4 \left(1 + \frac{\kappa_{Kr}}{\kappa_{es}}\right). \quad (33)$$

This yields for $\mu \equiv \nu \Sigma = \alpha \Omega_K h^2 \Sigma$ the result

$$\mu = \mathcal{K}^{1/3} \alpha^{4/3} \Sigma^{5/3} \Omega_K^{-2/3} C^{1/3}. \quad (34)$$

For the calculation of the equilibrium disc structure it is more convenient to write this relation in the form $\Sigma = \Sigma(\mu)$, because we know μ from Section 4, so

$$\Sigma = \mathcal{K}^{-1/5} \alpha^{-4/5} \mu^{3/5} \Omega_K^{2/5} C^{-1/5}. \quad (35)$$

We now discuss how to find the solution iteratively. First we calculate μ for given \dot{M} , B , etc., using equation (19), as discussed in the previous section. Next we find Σ using equation (35), where we assume $C = 1$ in the first iteration step. This allows us then to calculate h , ρ_c and T_c using equations (31) and (26) (assuming $\beta^{-1} = \beta_r^{-1} = 0$ in the first iteration step). We then calculate β^{-1} , β_r^{-1} , κ_{Kr} and thus k for the next iteration step.

Other iteration schemes are possible. For example one could iterate with respect to the opacity for electron scattering (instead of the Kramers opacity). Such an approach would converge faster in the outer parts of the disc, but it no longer converges near the disruption point.

In Fig. 3 we show $\Sigma(\varpi)$ for three different values of B . Note that Σ reaches a maximum at some value of ϖ and then it begins to decrease towards the neutron star. The profile of ρ_c is very similar and also has a maximum at approximately the same position as Σ . We shall see later that the location of this maximum coincides with the location where radiation pressure becomes important and where the disc becomes viscously unstable. Further inside this radius the thin-disc approximation is violated, because $h/\varpi > \mathcal{O}(1)$; see Fig. 4. Here, the temperature rises sharply; see Fig. 5.

To investigate the viscous stability of the solution we now

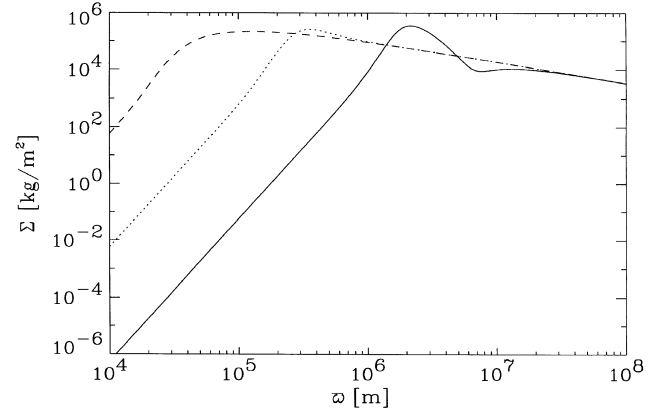


Figure 3. $\Sigma(\varpi)$ for three different values of B (solid line $B = 10^8$ T, dotted line $B = 10^6$ T and dashed line $B = 10^4$ T).

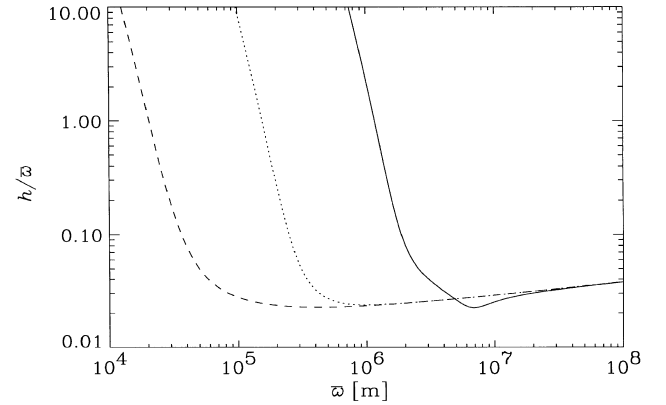


Figure 4. h/ϖ for three different values of B (solid line $B = 10^8$ T, dotted line $B = 10^6$ T and dashed line $B = 10^4$ T).

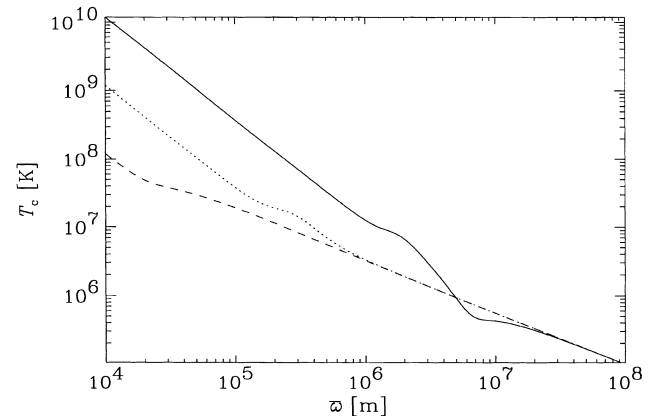


Figure 5. $T_c(\varpi)$ for three different values of B (solid line $B = 10^8$ T, dotted line $B = 10^6$ T and dashed line $B = 10^4$ T).

calculate the derivative $\partial \Sigma / \partial \mu$. In practice we calculate this derivative at each radius by calculating Σ for a slightly perturbed value of μ . When this derivative is positive the solution is viscously stable, otherwise it is viscously unstable. Following Heptinstall (1997) and Campbell & Heptinstall (1998), we associate the latter with the disruption of the disc. The result for $\partial \ln \Sigma / \partial \ln \mu$ is shown in Fig. 6. In Fig. 7 we plot β_r^{-1} , β^{-1} , and κ_{Kr}/κ_{es} for three different values of B

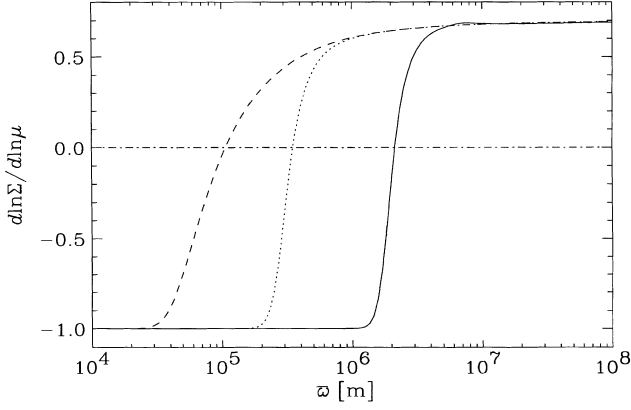


Figure 6. $\partial \ln \Sigma / \partial \ln \mu$ for three different values of B (solid line $B = 10^8$ T, dotted line $B = 10^6$ T and dashed line $B = 10^4$ T).

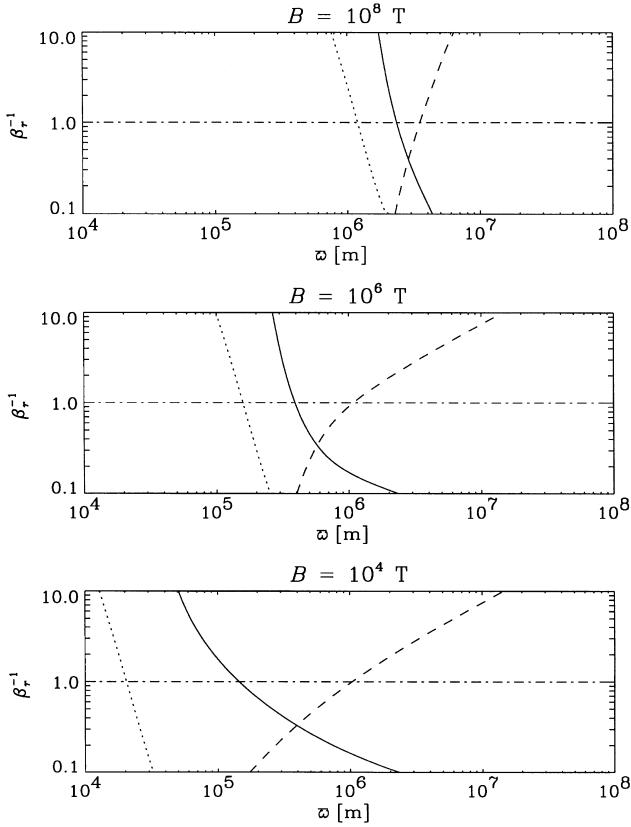


Figure 7. β_r^{-1} (solid line), β^{-1} (dotted line), and κ_{Kr}/κ_{es} (dashed line) for three different values of B .

as a function of ϖ . Note that the ordering where those three quantities become unity is unchanged in the parameter regime considered.

We note at this point that the magnetic field enters the problem mainly through equation (23) and thus (19). In the equations for mechanical and thermal equilibrium the magnetic field only becomes important when the magnetic pressure becomes comparable to the gas pressure. However, this is the case well inside the radius, where the disc becomes viscously unstable.

In Table 1 we give the disruption radius ϖ_{disr} where $\partial \Sigma / \partial \mu = 0$, and compare it with ϖ_{rad} where $P_{\text{rad}} = P_{\text{gas}}$, ϖ_{mag} where

Table 1. Summary of specific radii (in 10^6 m). For comparison, ϖ_A is 2.90, 0.209, and 0.015 times 10^6 m for $B = 10^8$, 10^6 and 10^4 T. In all cases $\varpi_{\text{co}} = 7.79 \times 10^6$ m. The asterisk in the last row refers to the solution discussed in Section 6.

B	$\hat{\epsilon}_{-2}$	α_{-2}	ϖ_{disr}	ϖ_{rad}	ϖ_{mag}	ϖ_{κ}	ϖ_z
10^8	1	1	2.13	2.34	1.19	3.49	1.87
10^6	1	1	0.35	0.39	0.16	1.08	0.25
10^4	1	1	0.11	0.15	0.02	1.03	0.04
10^8	10	1	1.36	1.50	0.44	2.47	1.13
10^8	.1	1	3.44	3.64	3.19	4.62	3.01
10^8	1	10	2.40	2.67	1.97	3.64	1.91
10^8	1	100	2.91	3.08	5.63	4.02	1.97
10^8	1	.1	2.00	2.18	0.73	3.46	1.92
10^8	10	10	1.45	1.61	0.73	2.49	1.19
10^8	100	100	0.97	1.11	0.44	1.75	0.68
10^8	3	1	1.72	1.89	0.74	2.97	1.47
10^8	*	1	1.62	1.82	–	3.04	1.30

$(B_{\phi}^{\pm})^2 / (2\mu_0) = P_{\text{gas}}$, ϖ_{κ} where $\kappa_{Kr} = \kappa_{es}$, and ϖ_z where $h/\varpi = 0.1$, i.e. where the thin-disc approximation breaks down.

The table shows that in all cases ϖ_{disr} is slightly smaller than ϖ_{rad} . Furthermore, ϖ_z is always smaller than ϖ_{disr} , so the thin-disc approximation still holds approximately near the disruption radius. Also, except for the case $\hat{\epsilon} = 10^{-3}$, ϖ_{mag} is always inside the disruption radius. This allows us to ignore the effect of the magnetic field in the relation $\Sigma = \Sigma(\mu)$. Likewise, ϖ_{κ} is always outside the disruption radius. Therefore, we can ignore the Kramers opacity near the disruption radius. Note that none of those approximations (except the thin-disc approximation) has been made so far. However, in the next section we derive an explicit analytic solution valid near the disruption radius. In order to do so we have to make a number of approximations that can be justified in the parameter range of interest.

5 ANALYTIC SOLUTION NEAR THE DISRUPTION RADIUS

The results above have shown that near the inner disruption point of the disc, i.e. where $\partial \Sigma / \partial \mu$ becomes negative, the solution is determined by electron scattering. Also, in the calculation of μ we can neglect \dot{M} , so equation (24) can be used. Substituting (24) into (35), and assuming $C = 1$ we obtain first Σ , and then h and T_c in the forms given below.

$$\Sigma = 7.2 \times 10^6 \alpha_{-2}^{-4/5} \hat{\epsilon}_{-2}^{-3/5} \varpi_6^{-27/10} R_4^{18/5} B_8^{6/5} M_{1.4}^{-1/10} \text{ kg m}^2, \quad (36)$$

$$h = 8.1 \times 10^4 \alpha_{-2}^{-1/10} \hat{\epsilon}_{-2}^{-1/5} \varpi_6^{7/20} R_4^{7/5} B_8^{2/5} M_{1.4}^{-9/20} \text{ m}, \quad (37)$$

$$T_c = 4.6 \times 10^7 \alpha_{-2}^{-1/5} \hat{\epsilon}_{-2}^{-2/5} \varpi_6^{-23/10} R_4^{12/5} B_8^{4/5} M_{1.4}^{-13/20} \text{ K}, \quad (38)$$

$$\beta^{-1} = 0.09 \alpha_{-2}^{9/10} \hat{\epsilon}_{-2}^{-6/5} \varpi_6^{-13/20} R_4^{6/5} B_8^{2/5} M_{1.4}^{-9/20}, \quad (39)$$

$$\beta_r^{-1} = 20 \alpha_{-2}^{1/10} \hat{\epsilon}_{-2}^{4/5} \varpi_6^{-77/20} R_4^{24/5} B_8^{4/5} M_{1.4}^{-13/20}, \quad (40)$$

$$\kappa_{es}/\kappa_{Kr} = 480 \alpha_{-2}^{8/5} \hat{\epsilon}_{-2}^{-1} \varpi_6^{-5} R_4^6 B_8^2 M_{1.4}^{-77/40}. \quad (41)$$

This is a useful approximation in the range $\varpi_{\text{rad}} \lesssim \varpi \lesssim \varpi_{\kappa}$. To calculate the range of validity we calculate ϖ_{rad} and ϖ_{κ} :

$$\varpi_{\text{rad}} = 2.2 \times 10^6 \alpha_{-2}^{2/77} \hat{\epsilon}_{-2}^{-16/77} R_4^{96/77} B_8^{32/77} M_{1.4}^{32/77} \text{ m}, \quad (42)$$

$$\varpi_{\kappa} = 3.4 \times 10^6 \alpha_{-2}^{8/25} \hat{\epsilon}_{-2}^{-1/5} R_4^{6/5} B_8^{2/5} M_{1.4}^{77/200} \text{ m}. \quad (43)$$

The range of validity collapses to zero when $\varpi_{\text{rad}}/\varpi_{\kappa} = 1$. From

equation (42) and equation (43) we obtain

$$\frac{\varpi_{\kappa}}{\varpi_{\text{rad}}} = 1.6\alpha_{-2}^{566/1925}\epsilon_{-2}^{3/385}R_4^{-18/385}B_8^{6/385}M_{1.4}^{-471/15400}. \quad (44)$$

The dependencies on $\hat{\epsilon}$, R , B and M are very weak. The strongest dependence comes through α . However, only for small values of α ($\alpha < 0.002$) would the range of applicability collapse to zero. Simulations of accretion-disc turbulence (Brandenburg et al. 1995, 1996) suggest that $\alpha \approx 0.01$ is a lower limit.

We should point out here that the simulations indicate that α depends on B and would therefore increase towards the inner parts of the disc. Again, this effect can be treated iteratively. The increase of α leads to an increase of β^{-1} which, according to equation (39), scales like $\alpha_{-2}^{9/10}$, so α becomes larger still. However, it is plausible to assume that α can never exceed a certain value around unity. Therefore we can read off the disruption radius directly from Table 1 assuming $\alpha_{-2} = 100$. This leads to a somewhat larger value: $\varpi_{\text{disr}} = 2.9 \times 10^6$ m. On the other hand, if $\hat{\epsilon}$ increases together with α , this leads to a somewhat smaller value: for $\alpha_{-2} = \hat{\epsilon}_{-2} = 100$ we have $\varpi_{\text{disr}} = 1.0 \times 10^6$ m.

Our analytic solution does not capture the turnover of the density at the point of instability. This is because radiation pressure is not included. If $P_{\text{rad}} > P_{\text{gas}}$, equation (35) would need to be replaced by

$$\Sigma = \left(\frac{4c}{9\kappa_{\text{es}}}\right)^2 \alpha^{-1} \Omega_{\text{K}}^{-1} \mu^{-1} \tilde{C}^{-2}, \quad (45)$$

where

$$\tilde{C} = \left(1 + \frac{16}{9}\text{Pr}_{\text{M}}^{-1}\beta^{-1}\right) \left(\frac{1 + \beta_{\text{r}}}{1 + \beta^{-1}}\right) \left(1 + \frac{\kappa_{\text{Kr}}}{\kappa_{\text{es}}}\right), \quad (46)$$

which is like the expression (33) for C , except that β_{r}^{-1} is now replaced by β_{r} . We see first of all that $\partial\Sigma/\partial\mu$ is *negative*, so the solution is viscously unstable. Secondly, from equation (24) we see that $\mu \propto \varpi^{-7/2}$, and so $\Sigma \propto \varpi^{+7/2}$. Thus, Σ indeed has a maximum and then falls off towards smaller radii.

6 SENSITIVITY TO THE η PRESCRIPTION

In this section we discuss the sensitivity of the results to the prescription of the magnetic diffusivity η adopted above. Instead of using (9) we now adopt

$$\eta = \text{Pr}_{\text{M}}^{-1} \alpha \Omega_{\text{K}} h^2, \quad (47)$$

with $\text{Pr}_{\text{M}} = 1$. Instead of equation (19) we have to integrate (3) explicitly, i.e.

$$\mu = \frac{\dot{M}}{3\pi} - \frac{4}{3\varpi^2 \Omega_{\text{K}}} \int_{\varpi}^{\infty} \varpi'^2 \frac{B_z B_{\phi}^+}{\mu_0} d\varpi'. \quad (48)$$

This can only be done once we know h . A few iterations suffice to calculate new values of Σ , h and μ . The result is shown in Fig. 8. Since $h/\varpi = \mathcal{O}(0.03)$ instead of 0.01 (see Fig. 4), we compare this result with the solution presented in Section 4 using $\hat{\epsilon}_{-2} = 3$. The various radii for the two solutions are given in the last two rows of Table 1.

It is important to note that the two results agree well outside the disruption radius. Also, μ still has a range where (24) is approximately valid, so the scaling behaviour of the disruption radius can still be described by (42). We also note that in this new solution β^{-1} never exceeds unity, as indicated by the dash in Table 1. This is because inside the disruption radius η is now larger and therefore B_{ϕ}^+ smaller. However, this result is not significant, because here the thin-disc approximation is no longer valid.

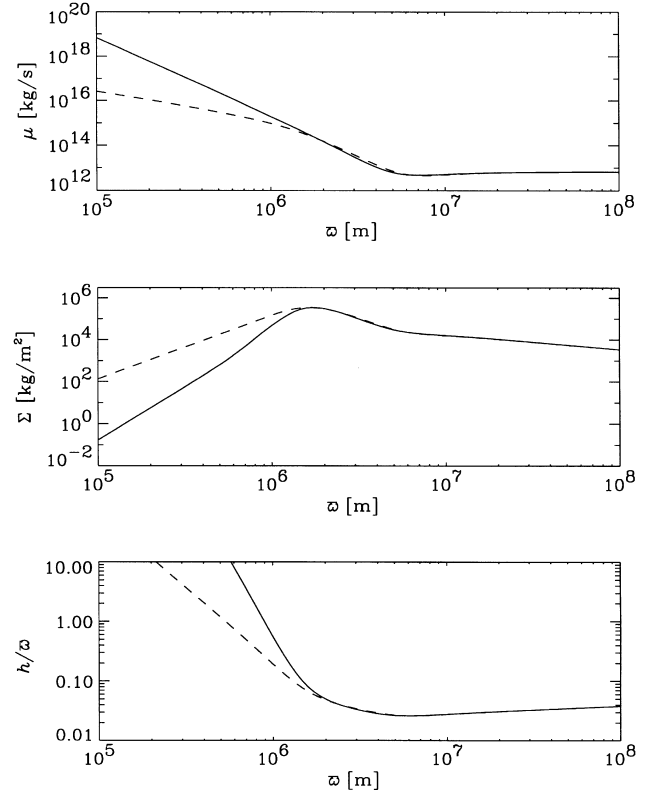


Figure 8. Comparison of μ , Σ and h/ϖ for two different magnetic diffusivity prescriptions: solid lines refer to (9) with $\hat{\epsilon} = 0.03$, whilst dashed lines refer to (47).

7 THE EFFECT OF VERTICAL MASS LOSS

Before the disc disrupts, most of the accreting matter must have been channelled along field lines towards the neutron star. This leads to an additional torque (Ghosh & Lamb 1979), which gives an extra term $-\varpi^3(\rho u_z)^+$ on the right-hand side of equation (3). Here, $(\rho u_z)^+$ is the vertical mass flux through the disc. With this additional term, equation (48) then becomes

$$\mu = \frac{\dot{M}}{3\pi} - \frac{4}{3\varpi^2 \Omega_{\text{K}}} \int_{\varpi}^{\infty} \left[\varpi'^2 \frac{B_z B_{\phi}^+}{\mu_0} - \varpi'^3 (\rho u_z)^+ \Omega \right] d\varpi'. \quad (49)$$

In the absence of a full solution for the magnetospheric flow we have to make some assumption about $(\rho u_z)^+$. The problem is similar to the stellar wind problem, but here the flow goes from the disc surface to the star. We assume that u_z^+ scales with the vertical Alfvén speed, $v_{\text{Az}} = \sqrt{B_z^2/(\mu_0 \rho^+)}$, and that ρ^+ is a small fraction of the density in the midplane, i.e. $\rho^+ = \lambda \rho_c = \lambda \Sigma/h$. Assuming that $\lambda = \text{constant}$, we can estimate λ from the constraint that the vertical mass loss of the disc must be equal to the accretion rate \dot{M} , i.e.

$$2 \int_{\varpi_{\text{disr}}}^{\infty} (2\pi \varpi') (\rho u_z)^+ d\varpi' = \dot{M}, \quad (50)$$

where the extra factor of 2 arises from the fact that mass is lost on both sides of the disc. Using the definitions of v_{Az} and Σ the integrand takes the form

$$4\pi \varpi' (\rho u_z)^+ = 2\pi R^3 \frac{B}{\sqrt{\mu_0}} \frac{1}{\varpi^2} \left(\frac{\lambda \Sigma}{h}\right)^{1/2}. \quad (51)$$

Thus,

$$\lambda = \left[\frac{2\pi R^3}{\dot{M}} \frac{B}{\sqrt{\mu_0}} \int_{\varpi_{\text{disr}}}^{\infty} \left(\frac{\Sigma}{h} \right)^{1/2} \frac{d\varpi'}{\varpi'^2} \right]^{-2}. \quad (52)$$

From the analytic solution of Section 5 we find

$$\lambda = 9 \times 10^{-10} \alpha_{-2}^{7/10} \hat{\epsilon}_{-2}^{2/5} \varpi_{6,\text{disr}}^{101/20} R_4^{-42/5} B_8^{-14/5} M_{1.4}^{-7/20}, \quad (53)$$

where $\varpi_{6,\text{disr}}$ is the disruption radius in 10^6 m. Substituting for $\varpi_{6,\text{disr}}$ the value ϖ_{rad} from (42), where radiation pressure becomes important, we obtain

$$\lambda = 5 \times 10^{-8} \alpha_{-2}^{64/77} \hat{\epsilon}_{-2}^{-50/77} R_4^{-162/77} B_8^{-54/77} M_{1.4}^{2693/1540}. \quad (54)$$

This value is close to the value $\lambda = 3 \times 10^{-8}$ obtained by integrating equation (49) numerically. Since the value of λ is so small, the results given in Table 1 are not affected by the inclusion of vertical mass loss.

8 THE SPIN-UP RATE

The solutions obtained allow us to calculate the torque exerted by the disc on the primary star. The resulting spin-up rate of the primary is given by

$$\frac{|\dot{P}|}{P} = -4\pi \int_{\varpi_{\text{disr}}}^{\infty} \varpi'^2 \frac{B_z B_\phi^+}{\mu_0} d\varpi' / \frac{2}{5} MR^2 \Omega_s \quad (55)$$

(Campbell 1997), where $P = 2\pi/\Omega_s$ is the rotation period of the star. The integral will be integrated numerically. The combined effects of spin-up and spin-down (from the outer regions where $\varpi > \varpi_{\text{co}}$) are then fully taken into account. The results for some parameter combinations are given in Table 2. However, in order to see the dependence of the result on the various parameters we now use (15) and assume $\varpi < \varpi_{\text{co}}$, which gives

$$\frac{|\dot{P}|}{P} = \frac{5}{6} \frac{PR^4}{M\varpi_{\text{disr}}^3} \frac{B^2}{2\mu_0 \hat{\epsilon}}. \quad (56)$$

Using equation (42) to estimate ϖ_{disr} we obtain

$$\frac{|\dot{P}|}{P} = 0.04 \alpha_{-2}^{-6/77} \hat{\epsilon}_{-2}^{-29/77} R_4^{20/77} B_8^{58/77} M_{1.4}^{-173/77} P_{10} \text{ yr}^{-1} \quad (57)$$

where P_{10} is the spin rate in units of 10 s. The resulting value of $|\dot{P}|/P$ is rather large compared with observed values, which are typically two orders of magnitude smaller. The main uncertainties in this result include the parameters α , $\hat{\epsilon} = \epsilon/\gamma$ and perhaps also B ; see Table 2.

9 CONCLUSION

The present investigations have shown that the disruption of the disc in the inner parts can be caused by a viscous instability, associated with radiation pressure and opacity due to electron scattering (cf. Lightman & Eardley 1974). The radial disc structure can be treated iteratively by an algebraic scheme as well as analytically in closed form, provided we assume that the magnetic diffusivity scales with the sound speed and the cylindrical radius (instead of the disc height).

We note that in the inner region, close to where the disc ends, the Maxwell stress essentially balances the viscous stress (i.e. $|F_{m\phi}| \approx |F_{v\phi}|$) with the small difference balancing the Reynolds stress. This occurs because the viscous force $|F_{v\phi}|$ becomes positive due to the magnetically modified radial variation of $\nu\Sigma$. The result that the disc ends where $|F_{m\phi}| \gtrsim |F_{v\phi}|$ confirms the work of Campbell (1992), and shows that this occurs for any plausible form of η .

Table 2. Summary of $|\dot{P}|/P$ for different combinations of α , γ and B_8 (i.e. the field in units of 10^8 T = 10^{12} G), using equation (49). The values of λ and ϖ_{disr} (in units of 10^6 m) are also given. In those cases where a value of λ is not given the effect of vertical mass loss is neglected, and equation (48) is solved instead. In all cases we used $\text{Pr}_M = 1$.

α	γ	B_8	$ \dot{P} /P$ [yr ⁻¹]	λ	$\varpi_{6,\text{disr}}$
0.01	0.03	1	4.7×10^{-2}	5×10^{-8}	2.0
0.01	0.01	1	2.2×10^{-2}	3×10^{-8}	1.6
0.01	0.001	1	3.7×10^{-3}	6×10^{-9}	1.1
0.1	0.01	1	4.6×10^{-3}	6×10^{-8}	1.2
1.0	0.01	1	8.8×10^{-4}	1×10^{-7}	0.9
1.0	0.001	1	1.8×10^{-4}	3×10^{-8}	0.6
1.0	0.001	1	7.4×10^{-5}	–	0.5
1.0	0.01	1	6.7×10^{-4}	–	0.8
1.0	0.01	0.1	6.9×10^{-5}	1×10^{-6}	0.4
1.0	0.01	0.1	7.5×10^{-6}	–	0.3

The analytic solution is surprisingly accurate, especially near the inner disruption radius. This solution proved to be useful in many respects (see Sections 7 and 8). Our main result is encapsulated in equation (42), which gives the radius ϖ_{rad} below which radiation pressure becomes important. This radius is approximately equal to ϖ_{disr} , the critical radius where the disc becomes viscously unstable. This radius can be associated with the inner disruption radius of the disc; see Table 1. This critical radius scales therefore with B like $\varpi_{\text{rad}} \propto B^{32/77} \approx B^{0.42}$. For $B = 10^4$ T the disruption point is close to the surface of the neutron star. In principle other physical effects could then become important, such as radial energy transport by advection. It is conceivable that even in the outer parts radial advection of energy could become important in certain parameter regimes. However, this has not yet been investigated.

Our disc solution seems to be relatively robust with respect to extra effects related to the coupling to the magnetosphere. For example the inclusion of a vertical mass loss from the wind has only a weak effect on the value of the disruption radius. Furthermore, our assumption of Keplerian rotation in the midplane is likely to be valid down to the disruption radius (Campbell 1992). Somewhere inside the disruption radius the angular velocity will undergo a transition from Ω_K to Ω_s . Again, we expect the actual location of the disruption radius to be insensitive to this.

The resulting spin-up rates are rather large compared with observations. However, some uncertainties in the parameters (most notably α , $\hat{\epsilon}$ and perhaps even B) could account for this. Indeed, turbulence simulations suggest that α (and probably also $\hat{\epsilon}$) increases with increasing field strengths to values close to unity (Hawley, Gammie & Balbus 1995, Brandenburg et al. 1996), which would lower the value of $|\dot{P}|/P$.

ACKNOWLEDGMENTS

We thank David Moss, Ulf Torkelsson and Vadim Urpin for useful criticism and suggestions.

REFERENCES

- Bardou A., Heyvaerts J., 1996, A&A, 307, 1009
 Basri G., Bertout C., 1989, ApJ, 341, 340
 Brandenburg A., Nordlund, Å., Stein R. F., Torkelsson U., 1995, ApJ, 446, 741
 Brandenburg A., Nordlund, Å., Stein R. F., Torkelsson U., 1996, ApJ, 458, L45

Campbell C. G., 1992, *Geophys. Astrophys. Fluid Dyn.*, 63, 179
Campbell C. G., 1997, *Magnetohydrodynamics in Binary Stars*. Kluwer, Dordrecht
Campbell C. G., Heptinstall P. M., 1998, *MNRAS*, in press
Ghosh P., Lamb F. K., 1979, *ApJ*, 232, 259
Hawley J. F., Gammie C. F., Balbus S. A., 1995, *ApJ*, 440, 742
Heptinstall P. M., 1997, PhD thesis, Univ. Newcastle upon Tyne

Lightman A. P., Eardley D. M., 1974, *ApJ*, 187, L1
Verbunt F., 1993, *ARA&A*, 31, 93
Warner B., 1995, *Cataclysmic Variable Stars*. Cambridge Univ. Press, Cambridge

This paper has been typeset from a $\text{T}_E\text{X}/\text{L}^A\text{T}_E\text{X}$ file prepared by the author.